J Nanopart Res (2013) 15:1705
DOI 10.1007/s11051-013-1705-3

RESEARCH PAPER

Poly(acrylic acid) coating induced 2-line ferrihydrite nanoparticle transport in saturated porous media

Aishuang Xiang · Weile Yan · Bruce E. Koel · Peter R. Jaffé

Received: 6 February 2013 / Accepted: 6 May 2013 / Published online: 22 June 2013

Abstract Iron oxide and iron nanoparticles (NPs) have been used effectively for environmental remediation, but are limited in their applications by strong retention in groundwater-saturated porous media. For example, delivery of NPs to large groundwater reservoirs would require large numbers of injection wells. To address this problem, we have explored polymer coatings as a surface engineering strategy to enhance transport of oxide nanoparticles in porous media. We report here on our studies of 2-line ferrihydrite NPs and the influence of poly (acrylic acid) (PAA) polymer coatings on the colloidal stability and transport in natural sand-packed column tests simulating flow in groundwater-saturated porous media. Measurements were also made of zeta potential, hydrodynamic diameter, and polymer adsorption and desorption properties. The coated NPs have a diameter range of 30–500 nm. We found that NP transport was improved by PAA coating and that the transport properties could be tuned by adjusting the polymer concentration. Our results demonstrate that a high stability of oxide particles and improved transport can be achieved in groundwater-saturated porous media by introducing negatively charged polyelectrolytes and optimizing polymer concentrations.

Keywords Polymer coating · Iron oxide nanoparticles · Ferrihydrite · Stability · Transport · Adsorption · Groundwater

Electronic supplementary material The online version of this article (doi:10.1007/s11051-013-1705-3) contains supplementary material, which is available to authorized users.

A. Xiang · B. E. Koel (✉)
Chemical and Biological Engineering Department, Princeton University, Princeton, NJ, USA
e-mail: bkoel@princeton.edu
URL: http://www.princeton.edu/cbe/people/faculty/koel/

W. Yan
Civil and Environmental Engineering, Texas Tech University, Lubbock, TX, USA

P. R. Jaffé (✉)
Civil and Environmental Engineering Department, Princeton University, Princeton, NJ, USA
e-mail: jaffe@princeton.edu
URL: https://www.princeton.edu/∼jaffe/

Introduction

Iron oxide nanoparticles (NPs) have many potential applications in environmental remediation efforts, including removing toxic chemicals and heavy metals from contaminated water (MacDonald et al. 2010). In one application of interest, uranium reduction and precipitation occur simultaneously with microbially mediated iron reduction, and so bioavailable iron oxides can enhance uranium remediation (Komlos et al. 2008). Poorly crystalline iron oxides such as ferrihydrite are highly reactive, binding with many contaminants and important nutrients in natural environments.

The practical use of iron oxide NPs involving well injection underground is severely limited, since the transport and delivery of iron oxide NPs at distances greater than a few meters in groundwater-saturated soil are a great challenge. Advances in surface engineering of these NPs are needed to increase stability and transport properties. While the colloidal properties and aggregation behavior of iron oxide particles have been studied (Wu et al. 2008; Chen 2007; Chibowski and Wiśniewska 2002), there are few investigations concerned with the influence of organic or polymer coatings on the stability of these NPs for environmental applications (Holsen et al. 1991; Ghosh et al. 2011). Surfactant coatings on ferrihydrite particle surfaces have been investigated to remove organic contaminants from water (Holsen et al. 1991), but no report has considered improving the delivery distance of ferrihydrite NPs in groundwater-saturated porous media by using organic or polymer coatings.

Poly(acrylic acid) (PAA) has been widely studied as a water-borne polyelectrolyte surface modifier for oxide NPs (Ghosh et al. 2011; Chibowski and Wiśniewska 2002). This polymer is a FDA-approved pharmaceutical additive (Orwoll and Yong 1999), and so it is a good candidate for surface engineering research in the environmental remediation. Such a polymer coating should strongly affect the stability and transport of iron oxide NPs. The adsorption of polyelectrolytes on NP surfaces determines the density and sign of charges on the surface of the resulting colloidal particles and affects their stability by changing the electrostatic and steric repulsion due to the attached polyelectrolyte layers. Charges on the surface of a solid depend significantly on the pH of the suspension. Measurements of the zeta potential (mV), a term derived from electric double layer theory (Hunter 1981), can be used to indicate NP stability.

In this paper, we report on studies of the stability and sorption of PAA coatings on 2-line ferrihydrite NPs with the goal of enhancing their transport and delivery in groundwater. Natural sand-packed column tests that simulate flow in groundwater-saturated porous media have been conducted with PAA-treated and non-treated 2-line ferrihydrite NPs. We find a remarkable increase in the transport distance of PAA-treated ferrihydrite NPs, matching that of trace sodium bromide in these column tests. Such performance has not been reported previously, and this surface engineering approach offers exciting prospects for improving the delivery of iron oxide NPs in saturated porous media.

Experimental methods

Nanoscale 2-line ferrihydrite nanoparticles

Synthesis of 2-line ferrihydrite nanoparticles followed a quick method reported previously (Schwertmann and Cornell 1991). First, 8 g $Fe(NO_3)_3{\cdot}9H_2O$ was dissolved in 100 mL DI water, and 66 mL 1 M KOH was added to bring the pH to 7–8 while vigorously stirring with a magnetic stirrer. The last 6 mL was added dropwise while constantly checking the pH. The mixture was stirred vigorously overnight, centrifuged, and rinsed with DI water four times. The solids were transferred into dialysis tubing and then dialysed quickly until free from electrolyte. The final particles were dispersed in DI water with a solid content of 10 g/L (counted as $Fe(OH)_3$), sonicated for 5 min, and stirred for 10 min, prior to storing at 5 °C for future use. The surface area of such synthesized 2-line ferrihydrite nanoparticles was 200–300 m^2/g (Schwertmann and Cornell 1991).

The stored 10 g/L ferrihydrite nanoparticles were stirred and sonicated well before each use in order to have a uniform dispersion. X-ray diffraction (XRD) analysis and transmission electron microscopy (TEM) were performed and compared with previous results (Schwertmann and Cornell 1991) in order to confirm that the our material was 2-line ferrihydrite nanoparticles.

Poly(acrylic acid)

Two sodium poly(acrylic acid) (PAA) polymers were applied as surface modifiers. Sodium PAA with molecular weight of 6,000 was supplied by Polysciences as a white powder (PAA6K, 100 % w/w). Sodium PAA with molecular weight of 140,000 and a solid content of 25 % (wt/wt) was supplied by Polysciences (PAA140K, with specific gravity of 1.1). Several stock solutions of 500–4,000 mg/L PAA6K and PAA140K were prepared, and these had pH values of 8–9 and a background electrolyte strength of 1–100 mM NaCl. All solutions in this study were made with deionized water unless otherwise stated.

Adsorption and desorption

Adsorption measurements were conducted in two ways: (1) dispersing synthesized 2-line ferrihydrite nanoparticles in PAA solutions and (2) synthesizing 2-line ferrihydrite nanoparticles in PAA solutions. A 15 mL sample of the coated NPs was centrifuged at a centrifugal acceleration of $10{,}410\times g$ and 20 °C for 30 min (DuPont Sorvall RC-5B refrigerated super speed centrifuge). The polymer concentration in the supernatant was analyzed by a total organic carbon (TOC) analyzer (Shimadu V-TOC/TN) in the non-purgeable organic carbon (NPOC) mode. The low-loading NPOC analysis was performed with 2 % 2 N HCl acid addition, 1.5 min sparge time, and 2–3 injections with a 50 μL injection volume. Other settings were kept as default values.

In the first method, an aliquot of stock solutions of 2,000 or 4,000 mg/L PAA and 10 mM NaCl was added to 20 mL scintillation vials to give a final polymer concentration from 25 to 1,800 mg/L, a background electrolyte of 10 mM NaCl, and a 2-line ferrihydrite nanoparticle solid content of 2.5 g/L. The electrolyte strength was balanced with 10 and 100 mM NaCl. A small volume of the 10 g/L 2-line ferrihydrite NP stock solution was injected into the polymer solution slowly with vigorous stirring. The coated NP samples were placed in an incubator (Fisher low temperature incubator model 307) at 20 °C for 24 h before centrifuging and NPOC analysis. The effect of PAA6K concentration on adsorption was studied at a pH of 3 and 10, as well as the effect of molecular weight on adsorption at a pH of 3 for various polymer concentrations.

Repeated coatings were applied to determine the maximum amount of polymer that could be coated on 2-line ferrihydrite nanoparticles at a pH of 8. In this procedure, 5 mL of the 10 g/L 2-line ferrihydrite suspension was injected with stirring into a small volume of the polymer stock solution to give a final polymer concentration of 500 mg/L and a solid content of 2.5 g/L. The rest of the coating and centrifuging procedure followed as described above. After centrifuging, aliquots of 500 mg/L polymer stock solution were added stepwise to the solids in order to recoat and disperse the 2-line ferrihydrite particles uniformly. The centrifuging and recoating were repeated 5 times. All coated samples contained 100 mM NaCl background electrolyte. The total organic carbon in each supernatant was determined by NPOC analysis. The maximum amount of polymer that could be coated on the surface was estimated from mass balance calculations.

In the second method, 2-line ferrihydrite NPs were synthesized in a 1,500 mg/L polymer solution with 100 mM NaCl. The volume of polymer solution contained more than the maximum amount of polymer that was coated on the NPs using the first method. Polymer was added to the synthesis solution before the NP synthesis step involving titration using 1 M KOH, and the solution was stirred well throughout. Otherwise, the synthesis procedures used were the same as in the synthesis of the bare 2-line ferrihydrite nanoparticles. The resulting solid content was 2.5 g/L. The amount of polymer adsorption on the particle surfaces was analyzed after centrifuging samples and measuring polymer concentrations in the supernatants with NPOC analysis.

The desorption of coated polymers from particle surfaces was investigated by repeatedly redispersing centrifuged solids in 100 mM NaCl. The process was the same as that used for the repeated coatings on bare (non-coated) 2-line ferrihydrite nanoparticles except that the polymer stock solution was replaced by 100 mM NaCl. Polymer content in the supernatant was determined with NPOC analysis. The amount of polymer that desorbed (was removed from) the particle surface was calculated by mass balance after each redispersion. Desorption was tested for samples that had maximum coating at the NP surface, i.e., NPs that had been repeatedly coated three times in the first procedure, as well as NPs synthesized in the polymer solutions in the second procedure.

DLS and zeta potential measurements

Dynamic light scanning (DLS) and electrophoretic light scanning (ELS) measurements of bare and coated 2-line ferrihydrite nanoparticles were performed for particle sizing and zeta potential using a Malvern Zetasizer Nano instrument. Ionic strengths of 1, 10, and 100 mM NaCl were utilized in bare 2-line ferrihydrite nanoparticle solutions with various pH values. Polymer coating on 2-line ferrihydrite nanoparticles occurred 12 h before analysis. The ratio of total polymer to solid content was varied at various pHs with a fixed electrolyte strength of 10 mM NaCl. The coating process followed the same procedure as

the adsorption test except that the 2-line ferrihydrite solid content was fixed at 50 mg/L. The final samples for DLS and ELS experiments were sonicated in a bath for 2 min and stirred continuously prior to measurement. Three zeta potential and particle size measurements were performed for each sample and the measurements were taken for at least two independent samples.

Porous matrix

Natural quartz ASTM sands were supplied by sigma-aldrich and used to simulate a groundwater-saturated porous matrix. The sand grains were spheroidal with a size range of 20–30 mesh. The treatment of this sand before packing it in the columns (described below) followed that described previously (Tiraferri and Sethi 2009). The grains were soaked in 6 N HCl for 72 h and subsequently rinsed in deionized water to restore the initial pH. Prior to packing the column, the grains were rehydrated by boiling them in DI water for 20 min. The soaked sand grains were sonicated in DI water for 25 min to remove detachable colloids. The grains were washed again and dried in an oven at 120 °C. The dried sand matrix total porosity was measured to be 0.37 (as described later).

Column transport experiments

Glass chromatography columns (Knotes Brand Chromaflex) with an inner diameter of 2.5 cm and a fixed length of 15 cm were used in column transport experiments. Dry sand grains were wet packed with vibration to minimize any layering or air entrapment. The pore volume for each column was 27.45 mL. The transport experiments were conducted using vertical columns by pumping a suspension of 2-line ferrihydrite nanoparticles from the bottom to the top using a peristaltic pump (Ismatec® low-speed planetary gear-driven digital pump) at an approach velocity of 1.08×10^{-5} m/s. Prior to each experiment, the packed column was equilibrated by flushing the porous matrix with 10 pore volumes of pH-adjusted DI water and 10 pore volumes of pH-adjusted 10 mM NaCl electrolyte solution.

Samples of 800 mL of the influent suspension were prepared by injection of 10 g/L bare 2-line ferrihydrite nanoparticles into a pretreated solution while stirring. The pretreated solution had a pH of 6.5, a background electrolyte concentration of 10 mM NaCl, and various amounts of dissolved PAA6K with an initial concentration range from 0 to 500 ppm. An initial concentration of 500 ppm, for example, results in only 5 % of the PAA6K remaining in solution after equilibration. The influent solution to the column experiments contained this dissolved PAA6K in equilibrium with the nanoparticles. The final 2-line ferrihydrite nanoparticle solid content was 150 mg/L as calculated from the chemical formula of $Fe(OH)_3$. The suspension was stabilized 24 h at room temperature with stirring and the pH readjusted to 6.5 prior to pumping into the column. The suspension was kept stirring at a speed of 300 rpm during the transport test.

The effluent at the column outlet was collected with a fraction collector (Spectra/Chrom®CF-2) at a frequency of 30 min for the first 10 samples and 60 min for rest of the samples. The particle concentration in the fractions was monitored using a previously reported spectrophotometric iron analysis method (Komlos and Jaffé 2004). In our procedure, 1 mL sample was added into 4 mL 0.65 N HCl. The mixture was mixed well and left at the room temperature for 1 h in order to completely dissolve the iron. 0.2 mL 6.25 N hydroxylamine hydrochloride was then added to reduce ferric ions into ferrous ions. This was kept overnight before transferring a 0.1 mL sample into 5 mL 1 g/L ferrozine buffered with 11.92 g/L HEPES (4-(2-hydroxyethyl)-1-piperazineethanesulfonic acid). The absorbance was read from a spectrophotometer (Spectronic®Genesys™ 2) at a wavelength of 562 nm.

Results and discussion

Two methods were examined to manufacture the PAA-coated 2-line ferrihydrite nanoparticles. The first method consisted of coating the nanoparticles after synthesis and the second method consisted of synthesizing the nanoparticles directly in the polymer solution. Table S1 compares the maximal polymer adsorption for the two coating strategies starting with an equivalent amount of PAA in the initial coating solution. Synthesis of the nanoparticles in the polymer solution resulted in a higher polymer loading. The higher polymer loading is possibly because the polymer was incorporated into the matrix of the NPs during the synthesis in the polymer solution. Since the

measurements of particle size and zeta potential for the two types of nanoparticles gave negligible differences, the work described here utilizes only method of coating the nanoparticles after synthesis.

Stability

Stability of colloidal particles depends notably on the pH of the solution. Electrolyte ion strength also plays a role in affecting colloid stability. Typical ground waters have concentrations of monovalent cations of up to 10 mM, and their aquifer pH ranges between 6 and 8. Groundwater-saturated porous media usually is negatively charged, i.e., has a negative zeta potential.

Figure 1 shows the influence of monovalent cations and pH of the solution on the zeta potential of bare 2-line ferrihydrite nanoparticles. Much of the uncertainty in these curves comes from changes in pH that occurred from the lack of buffering capacity. Figure 1 demonstrates that electrolyte strength has a negligible effect on the zeta potential of these nanoparticles. The point of zero zeta potential (pH_{iep}) for all of these nanoparticles is between 8 and 8.5. This number matches the literature point of zero charge of about 8 (Cornell and Schwertmann 2003). Figure 1 also indicates that the zeta potential depends significantly on the pH of the suspension. A positive zeta potential is induced by the positive surface charge on the particle surface at low pH. High pH values restrict iron oxide surface ionization and the adsorption of anions leads to negative zeta potentials. Bare 2-line ferrihydrite nanoparticles are positively charged at a pH of 6–8 suggesting that they would strongly adsorb onto groundwater-saturated porous media.

Hydrodynamic diameter is another indicator of nanoparticle stability. Figure 2 presents the influence of suspension pH and background electrolyte strength on the nanoparticle hydrodynamic diameter. The maximum particle size occured at a pH near the point of zero charge (between eight and nine) for all of these electrolyte strengths. We found the hydrodynamic diameter to not be linear with the electrolyte strength, but this diameter is known to be sensitive to the time spent in the colloidal suspension with an electrolyte background (Ghosh et al. 2011).

A polymer coating was applied to the nanoparticles and Figs. 3 and 4 present results of zeta potential and hydrodynamic diameter measurements for these

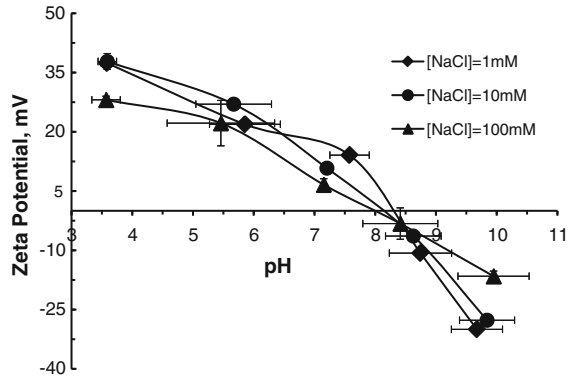

Fig. 1 The effect of background electrolyte and pH on the zeta potential of 2-line ferrihydrite particles at a solid content of 50 mg/L

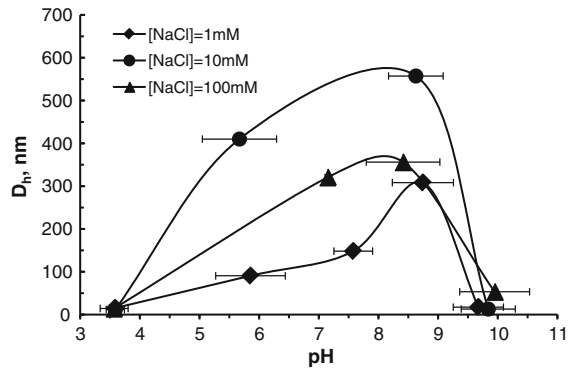

Fig. 2 The effect of background electrolyte and pH on the hydrodynamic diameter of 2-line ferrihydrite particles at a solid content of 50 mg/L. The *vertical error bars* are smaller than the *data point symbols*

PAA-coated 2-line ferrihydrite nanoparticles. The zeta potential of the NPs with adsorbed PAA is lower than the potential for the bare NPs in the examined pH range (Figs. 1 and 3). The negatively charged $–COO^-$ groups distributed along the polymer chains cause this lowering of the zeta potential. PAA coating also shifts the point of zero zeta potential (pH_{iep}) to lower pH values, and this shift depends on the PAA concentration. The dependence of the zeta potential on the molecular weight of the PAA used is negligible in the studied polymer concentrations. One reason for this is that the nanoparticle surface area is much greater than other iron oxide particles and this may cause polymer molecules with different molecular weights to adopt similar conformations on the particle surface.

A detailed discussion has been reported for zeta potential shifting of Fe_2O_3 iron oxide with various

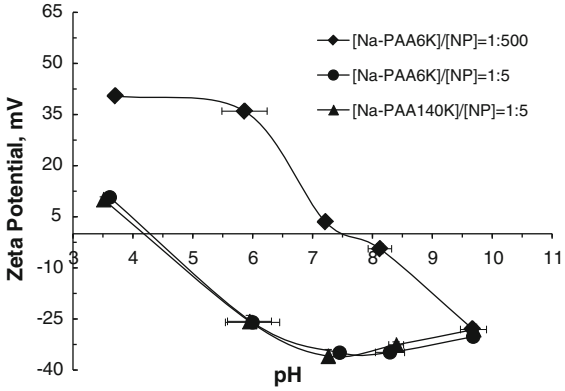

Fig. 3 The effect of PAA and pH on the zeta potential of 2-line ferrihydrite particles at a solid content of 50 mg/L and sodium strength of 10 mM. The *vertical error bars* are smaller than the *data point symbols*

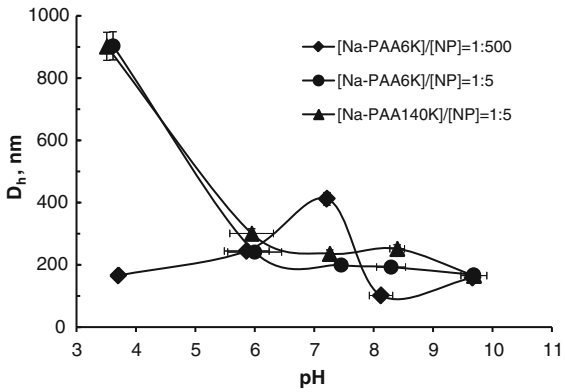

Fig. 4 The effect of PAA and pH on the hydrodynamic diameter of 2-line ferrihydrite particles at a solid content of 50 mg/L and sodium strength of 10 mM

PAA concentrations and molecular weights (Chibowski and Wiśniewska 2002). Generally, three possible effects change the zeta potential of polymer-coated iron oxide particles: (i) conformation of the polymer chains might move the slipping plane (M'Pandou and Siffert 1987), (ii) active sites might be blocked on the particle surface (Tjipangandjara and Somasundaran 1991), and (iii) charged functional groups in chains of adsorbed polymer may alter surface charge (Chibowski et.al. 2000). The negligible effect of the polymer molecular weight on the zeta potential suggests that the length and number of tails and loops formed at the interface are the same and so do not affect the zeta potential of iron oxide. However, since increasing the polymer concentration leads to larger and more numerous tails and loops formed at the surface, the zeta potential shifts to negative values with sufficient negative functional groups at the interface.

Figure 4 demonstrates that larger hydrodynamic diameters were observed for various polymers and concentrations at pH values near pH_{iep}. Minimum diameters occur at maximum absolute zeta potentials. Oxide particles in suspensions with high absolute zeta potentials do not aggregate at a fast pace, and they have small hydrodynamic diameters. Thus, stability of these particles within a targeted pH range can be improved by applying PAA coatings.

These studies demonstrate that the zeta potential of oxide particles in groundwater (pH = 6–8, and <10 mM monovalent concentration) can be tuned to a significantly negative value that results in good stability in a negatively charged porous media.

Adsorption and desorption

Because the amount and nature of organic matter introduced into groundwater with the nanoparticles are strictly regulated, it is important to control the organic matter content in applying polymer coatings to nanoparticles used for environmental remediation. Figure 5 presents adsorption isotherms of PAA on the surface of 2-line ferrihydrite nanoparticles. This figure illustrates the influence of the PAA molecular weight and pH of the solution on PAA adsorption on these nanoparticles.

Compared to results from adsorption isotherms of PAA on hematite iron oxide particles at the same pHs

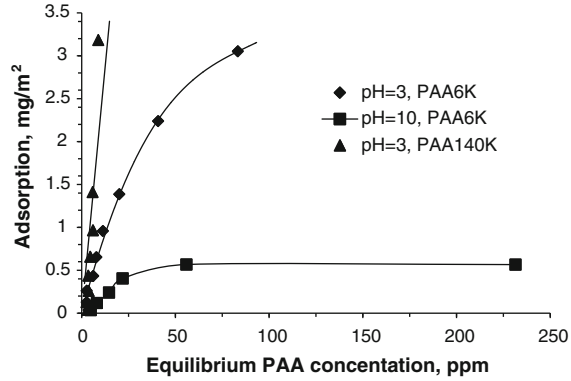

Fig. 5 Adsorption isotherms of PAA on 2-line ferrihydrite nanoparticles for two molecular weights of the polymer and two values of pH. [NaCl] = 10 mM, [2-line ferrihydrite] = 2.25 g/L, and the other two *solid curves* are the fittings to the experimental data

of 3 and 10, respectively (Chibowski and Wiśniewska 2002), 2-line ferrihydrite nanoparticles have much greater capacity per unit surface area for adsorption of PAA. This is because 2-line ferrihydrite nanoparticles have higher cationic surface charge than hematite particles at these pH values, and therefore can absorb more PAA, a polyelectrolyte that contains carboxylic groups.

A detailed discussion of the influence of PAA molecular weight and pH of the solution on the adsorption isotherms of PAA on hematite has been presented (Chibowski and Wiśniewska 2002). Our results on 2-line ferrihydrite nanoparticles confirm that the increase of polymer molecular weight gives more polymer adsorption in the studied equilibrium polymer concentration range. However, we saw no significant difference in the isotherms for PAA6 and PAA140K at pH = 3 up to an adsorption of 0.6 mg/m^2. At higher polymer concentration, long loops and tails or greater number of these structures are formed with higher molecular weight polymer at the interface of oxide particles; therefore, increased amount of adsorption is observed for high molecular weight polymer. The value of 0.6 mg/m^2, below which there is no influence of polymer molecular weight, is three times greater than that value for hematite nanoparticles, and so the range of efficient coating using low molecular weight polymers is extended.

The increase of pH from 3 to 10 for the PAA6K isotherms as shown in Fig. 5 causes a large decrease in PAA adsorption. The solution pH affects the degree of ionization of the PAA carboxylic groups, such that as the pH is decreased below the value of pK_a = 4.5, more non-dissociated carboxylic groups, –COOH, are induced than dissociated ones, –COO$^-$, and with an increase of pH greater than 4.5, the number of –COO$^-$ groups in the polymer chains increase. It hinders interaction of the polymer with more and more negatively charged surface of oxide particles and thus decreases the adsorption of PAA (Chibowski and Wiśniewska 2002).

Once injected into groundwater and during their transport through a porous medium, polymers adsorbed to the oxide particle surfaces may detach, decreasing the stability of the oxide nanoparticles. In order to probe the stability of the polymer coating, we carried out measurements of PAA desorption from the maximally coated 2-line ferrihydrite nanoparticles after synthesis. First, a maximum coating strategy was pursued. Figure 6 presents our determination of the number of coating treatments required to achieve maximal polymer coating on the nanoparticles. In this figure, a normalized total organic carbon (TOC) value, obtained from the TOC value in the supernatant solution after a coating treatment, was divided by the TOC value in the original polymer solution. This value is plotted versus the number of coating treatments as shown in Fig. 6. When the normalized TOC reaches a value of unity, no additional polymer adsorption occurs with further treatment. The maximal coating was achieved after 2–3 coating treatments for both PAA6 and PAA140K.

PAA desorption was measured by repeatedly dispersing the maximally coated 2-line ferrihydrite nanoparticles 4 times in a 100 mM NaCl solution. Figure 7 shows the polymer desorption caused by these repeated dispersions. The amount of polymer desorption observed after four repeated dispersions was 2 % for PAA140K and 5 % for PAA6K. The lower desorption of PAA140K can be explained by the higher adsorption isotherms for this polymer as shown in Fig. 5. Figure 7 also shows that a higher loading of adsorbed polymer leads to a higher amount of polymer desorption when contacting a fresh solution.

Transport

When injected into natural aquifers, highly concentrated slurries of iron oxide nanoparticles will need to

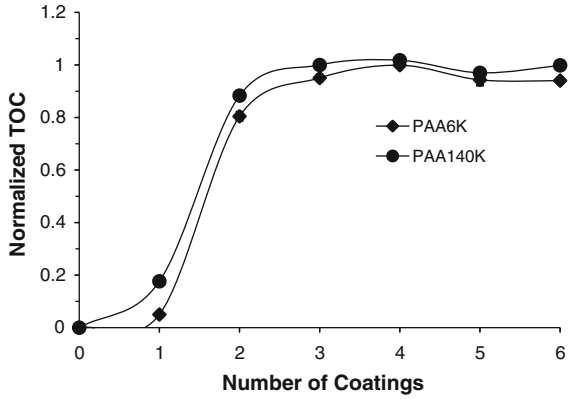

Fig. 6 A normalized total organic carbon (TOC) value in the supernatant solution was measured after each repeated coating/centrifuging step to track the extent of polymer adsorption on previously prepared nanoparticles

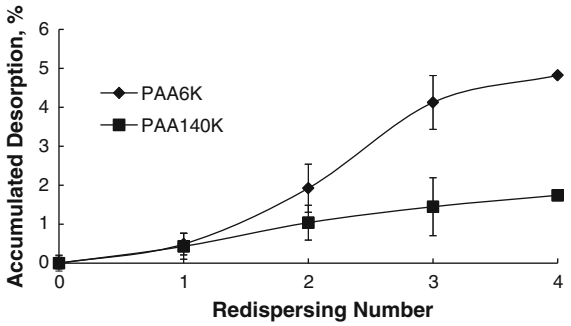

Fig. 7 Polymer desorption measurements using multiple redispersions in 100 mM NaCl for polymer coatings added after the NP synthesis. The initial particle, prior to any desorption is plotted on the origin. Each *vertical error bar* represents an accumulation of errors from previous samples

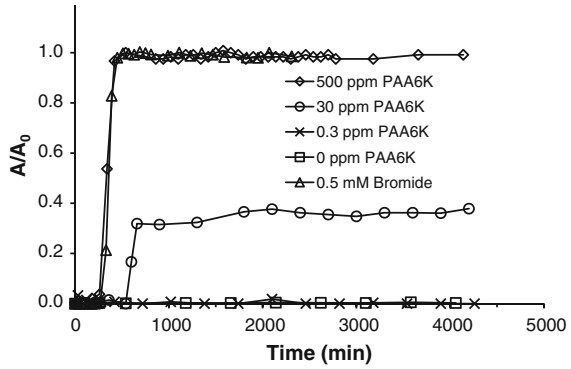

Fig. 8 Transport measurements through natural quartzs and columns showing *breakthrough curves* of 2-line ferrihydrite nanoparticles that have been coated by PAA6K using various polymer solution concentrations. The bromide *breakthrough curve* provides a reference for a solute that is not interacting with the *solid matrix*. The nanoparticle feed solution was controlled to be pH = 6.5

move from wells to the contaminated zone or spread to embrace the source of contamination. These distances are not likely to be less than tens of meters or more than hundreds of meters (Tiraferri and Sethi 2009). Bare iron oxide nanoparticles do not have sufficient mobility for many applications. We have shown that PAA coatings alter the zeta potential to indicate enhanced nanoparticle stability. However, direct transport measurements using the coated nanoparticles are necessary to obtain data needed for predicting transport distances.

Figure 8 reports our transport measurement results through 15-cm long, 2.5-cm inner dia. columns packed with negatively charged natural quartz sands. This figure presents breakthrough curves of 2-line ferrihydrite particles with various amounts of PAA6K coatings (applied subsequent to the NP synthesis). A breakthrough curve for bromide (added as sodium bromide) is also provided as a reference for transport of a conservative tracer that has no interaction with the solid phase. As shown in Fig. 8, bare or minimally PAA6K-coated 2-line ferrihydrite nanoparticles are not transported through the column. However, nanoparticles coated extensively using a 500 ppm PAA6K coating solution have a breakthrough curve showing transport as facile as bromide for the testing period. Oxide particles coated with moderate amounts of PAA6K polymer are only partially transported through the column. The transport of particles coated with PAA140K should be similar to these results, since particles coated with PAA6K have similar zeta potential to particles coated with PAA140K at a solution pH of 6.5 (Fig. 3).

Zeta potential measurements show negative values for suspensions with 500 and 30 ppm PAA6K coatings (−35 to −40 mV), and positive values for those with 0 and 0.3 ppm PAA6K coatings (5–10 mV). Our transport results demonstrate that nanoparticle suspensions with positive zeta potentials are not transported through columns packed with negatively charged natural quartz sands. However, suspensions with negative zeta potentials may be fully or partially transported through the columns depending on the amount of polyelectrolyte in the coating on the oxide particles.

We also measured the zeta potential and hydrodynamic diameter of the 500 ppm PAA6K-coated nanoparticle fractions that were transported through the test column. D_H stayed in a range of 245–255 nm for all collected fractions, and the zeta potential was nearly constant, decreasing only 3 mV in the testing period. All of these results indicate that suspensions formed using 500 ppm PAA6K are stable in this porous sand media. This finding is a promising advance toward our goal of achieving sustainable delivery of iron oxide nanoparticles in groundwater.

Predicting the nanoparticle travel distance, i.e., the distance where 99 % of the particles are removed, is a challenge. According to a methodology that used an attachment efficiency in calculations of the travel distance for zero valent iron nanoparticles coated with guar gum (Tiraferri and Sethi 2009), we conclude that our 2-line ferrihydrite nanoparticles coated in

500 ppm PAA6K have zero attachment efficiency. However, such suspensions are not expected to travel an infinite distance in such porous media because of gradual desorption of polymer from the NP surface during transport over long distances or time, which reduces the mobility.

Conclusions

Polymer coatings as a surface engineering strategy have been explored to enhance transport of iron oxide nanoparticles in the groundwater-saturated porous media. Our studies of 2-line ferrihydrite NPs and the influence of PAA polymer coatings on transport through the natural quartz packed columns reveal that improved transport can be achieved in the groundwater-saturated porous media by introducing negatively charged polyelectrolytes and optimizing polymer concentrations. The nanoparticles coated extensively using a 500 ppm or greater amount of PAA6K coating solution may approach the transport performance of tracer bromide since they have breakthrough curves as facile as bromide for the testing period.

Our studies confirmed that the measurement of zeta potential can be a good tool to indirectly determine the stability of the polymer-coated NPs in the porous media, and that the value of zeta potential of the NP suspension can be an effective criterion in selecting the coating polymers. Zeta potential of oxide particles with polymer coatings can be tuned to a significantly negative value that results in good stability in a negatively charged porous media. The nanoparticle suspensions with positive zeta potentials are not transported through columns packed with negatively charged natural quartz sands. However, suspensions with negative zeta potentials can be fully or partially transported through the columns depending on the amount of polyelectrolyte in the coating on the oxide particles.

The desorption properties of the coating polymer on the NPs should be carefully considered. Significant amount of polymer desorption would require large amounts of initially adsorbed polymers to enhance the nanoparticle stability over longer transport distances, which increases the amount of organic matter introduced into the environment and the cost of the remediation strategy.

Acknowledgments The authors acknowledge support of the Andlinger Innovation Fund of the Andlinger Center for Energy and the Environment at Princeton University. The authors thank Prof. Robert Prud'homme for his valuable discussions and his group for assistance.

References

Chen S (2007) Polymer-coated iron oxide nanoparticles for medical imaging. PhD thesis, Massachusetts Institute of Technology

Chibowski S, Wiśniewska M (2002) Study of electrokinetic properties and structure of adsorbed layers of polyacrylic acid and polyacrylamide at Fe_2O_3–polymer solution interface. Colloids Surf A 208:131–145

Cornell RM, Schwertmann U (2003) The Iron oxides: structure, properties, reactions, occurrences and uses, 2nd ed. Wiley-VCH, New york

Ghosh S, Jiang W, McClements JD, Xing B (2011) Colloidal stability of magnetic iron oxide nanoparticles: influence of natural organic matter and synthetic polyelectrolytes. Langmir 27:8036–8043

Holsen TM, Taylor ER, Seo YC, Anderson PR (1991) Removal of sparingly soluble organic chemicals from aqueous solutions with surfactant-coated ferrihydrite. Environ Sci Technol 25:1585–1589

Hunter RJ (1981) Zeta potential in colloid science: principles and applications. Academic Press, New York, pp 20–85

Komlos J, Jaffé PR (2004) Effect of iron bioavailability on dissolved hydrogen concentrations during microbial iron reduction. Biodegradation 15:315–325

Komlos J, Peacock A, Kukkadapu RK, Jaffé PR (2008) Long-term dynamics of uranium reduction/reoxidation under low sulfate conditions. Geochim Cosmochim Acta 72(15): 3603–3615

M'Pandou A, Siffert B (1987) Polyethyleneglycol adsorption at TiO_2–H_2O interface: distortion of ionic structure and shear plane position. Coll Surf 24:159–172

Macdonald LH, Moon HS, Jaffé PR (2011) The role of biomass, electron shuttles, and ferrous iron in the kinetics of geobacter sulfurreducens-mediated ferrihydrite reduction. Water Res 45:1049–1062

Orwoll RA, Yong CS (1999) Polymer Data Handbook. Oxford University Press, Newyork, pp 252–253

Tiraferri A, Sethi R (2009) Enhanced transport of zero valent iron nanoparticles in saturated porous media by guar gum. J Nanopart Res 11:635–645

Wu W, He Q, Jiang C (2008) Magnetic iron oxide nanoparticles: synthesis and surface functionalization strategies. Nanoscale Res Lett 3:397–415